Robustness of fragmented condensate many-body states for continuous distribution amplitudes in Fock space

Uwe R. Fischer and Bo Xiong

Seoul National University, Department of Physics and Astronomy, Center for Theoretical Physics, 151-747 Seoul, Korea

(Received 18 June 2013; published 4 November 2013)

We consider a two-mode model describing scalar bosons with two-body interactions in a single trap, taking into account coherent pair exchange between the modes. It is demonstrated that the resulting fragmented many-body states with continuous (nonsingular) Fock-space distribution amplitudes are robust against perturbations due to occupation number and relative phase fluctuations, Josephson-type tunneling between the modes, and weakly broken parity of orbitals, as well as against perturbations due to interaction with a third mode.

DOI: 10.1103/PhysRevA.88.053602 PACS number(s): 03.75.Hh, 03.75.Nt, 03.75.Lm

I. INTRODUCTION

Conventional wisdom has it that fragmented condensates, i.e., many-body states leading to more than one macroscopic eigenvalue of the single-particle density matrix [1], are unstable against small perturbations when contained in a single (e.g., harmonic) trap [2,3]. It is well established that stable fragmentation can be readily prepared for spatially well separated modes in the field operator expansion, for example, in deep double wells [4] or in optical lattices [5–7]. On the other hand, fragmented condensate states in a single trap are conventionally obtained around special points of symmetry of the system, e.g., in spin-1 Bose gases [8,9], rotating gases [10–13], and spin-orbit-coupled systems [14]. These fragmented condensate many-body states obtained from symmetry in a single trap are sharply peaked in Fock space; as a consequence, they are inherently unstable against perturbations and decay into single condensates. Recent theoretical work, however, put forward the possibility of *robust* fragmented condensate states in a single trap, with significant (that is, not exponentially small) spatial overlapping of the field operator modes [15]. The corresponding class of fragmented condensate many-body states was subsequently shown to be immune against perturbations on the dynamical many-body level, i.e., under rapid changes of interaction couplings [16].

In what follows, we elucidate the distinct features of the ground-state many-body properties of stably fragmented condensates by contrasting them with the fragility of symmetry-point-induced fragmented condensate states. To this end, and to illustrate the salient features of stable fragmentation for interacting bosons in a most transparent fashion, we use a simple model with just two macroscopically occupied field operator modes. Within this model, a closed analytical expression for fragmented condensate many-body states can be devised. Using the corresponding many-body amplitudes in Fock space, we demonstrate that a fragmented state with *continuous* (i.e., nonsingular) probability amplitudes for the Fock basis states is stable against quantum fluctuations of the occupation numbers of the modes and their relative phase, as well as against single-particle tunneling between the two states. We contrast this with the well-known instability of symmetry-point-induced fragmented states, which occurs in our model at vanishing pair-exchange coupling. In addition, we investigate whether a (slightly) broken parity of orbitals significantly influences fragmentation. Finally, we discuss the perturbative effect of introducing an additional interacting mode. We find that the single-particle density matrix has essentially still two macroscopic eigenvalues, and the many-body state thus remains twofold fragmented.

II. TWO-MODE FRAGMENTED STATES

A. Hamiltonian and the many-body states

We describe the quantum many-body phases of interacting bosons by the following two-mode Hamiltonian [15]:

$$\hat{H} = \sum_{i=0,1}\left[\epsilon_i \hat{n}_i + \frac{U_i}{2}\hat{n}_i(\hat{n}_i - 1)\right] + \frac{P}{2}(\hat{a}_0^\dagger\hat{a}_0^\dagger\hat{a}_1\hat{a}_1 + \text{H.c.}) + \frac{V}{2}\hat{n}_0\hat{n}_1. \quad (1)$$

Without pair-exchange coupling, $P = 0$, for $U_0 + U_1 - V > 0$, we obtain a Fock state $|N_0,N_1\rangle$, where the particle number in the ground-state mode $N_0 = \frac{N}{2} - \frac{(U_0-U_1)(N-1)+2(\epsilon_0-\epsilon_1)}{2(U_0+U_1-V)}$. Here, $N = N_0 + N_1$ is the total number of particles. To obtain the generic features of the ground state for the Hamiltonian (1), we expand in a linear superposition of Fock states, $|\Psi\rangle = \sum_{l=0}^N \psi_l|l\rangle$, where $|l\rangle \equiv |N-l,l\rangle$ [15]. This Fock state expansion, by its definition, respects total particle number conservation, and the many-body correlations are encoded in the generally complex distribution vector $\psi_l = |\psi_l|\exp[i\theta_l]$, with amplitude $|\psi_l|$ and phase θ_l. The distribution satisfies, according to the Hamiltonian (1), the $N+1$ equations

$$\langle l|\hat{H}|\Psi\rangle = E\psi_l = \frac{P}{2}(d_l\psi_{l+2} + d_{l-2}\psi_{l-2}) + c_l\psi_l, \quad (2)$$

where the coefficients $c_l = \epsilon_0(N-l) + \epsilon_1 l + \frac{1}{2}U_0(N-l)(N-l-1) + \frac{1}{2}U_1 l(l-1) + \frac{1}{2}V(N-l)l$ and $d_l = \sqrt{(l+2)(l+1)(N-l-1)(N-l)}$.

Equations (2) decompose into two *independent* sets of equations containing the even and odd l sectors of ψ_l only. The two corresponding ground states in the even and odd l sectors are therefore *degenerate* in the continuum limit of $N \to \infty$.

To represent the structure of the many-body wave function sufficiently far away from the singular symmetry point $P = 0$, we employ the spinor wave functions [2]:

$$|\theta,\phi\rangle = \frac{1}{\sqrt{N!}}(u\hat{a}_1^\dagger + v\hat{a}_2^\dagger)^N|0\rangle, \quad (3)$$

where the coefficients read $u = e^{-i\phi/2}\cos(\theta/2)$ and $v = e^{i\phi/2}\sin(\theta/2)$. Due to the even and odd l sector degeneracy, the weights of even and odd sectors α and β, respectively, are arbitrary (subject to normalization of the wave function). Upon investigating the structure of the binomially expanded spinor wave-function basis above, taking into account the degeneracy of the even-odd l sector, we can write an ansatz for the many-body wave function in the form

$$|\Psi\rangle = \alpha\sqrt{\frac{2}{N!}}\sum_{k=0}^{N/2} C_N^{2k}(u\hat{a}_0^\dagger)^{2k}(v\hat{a}_1^\dagger)^{N-2k}|0\rangle + \beta\sqrt{\frac{2}{N!}}\sum_{k=1}^{N/2} C_N^{2k-1}(u\hat{a}_0^\dagger)^{2k-1}(v\hat{a}_1^\dagger)^{N-2k+1}|0\rangle, \quad (4)$$

where the binomial coefficients are $C_N^k = \frac{N!}{(N-k)!k!}$, $u = \exp[-i\phi_2/2]\cos(\theta/2)$, $v = \exp[i\phi_2/2]\sin(\theta/2)$ and ϕ_2 here represents half the phase difference between the l and $l+2$ modes, defined such as to enter identically for even and odd l sectors. We assume for simplicity that N is even.

The normalization of the wave function implies $|\alpha|^2 + |\beta|^2 = 1$. The phase relation between even and odd Fock states is defined by writing $\alpha = |\alpha|\exp[-i\phi_1/2]$ and $\beta = |\beta|\exp[i\phi_1/2]$. The matrix elements of the single-particle density matrix in this state are $\langle\Psi|\hat{a}_0^\dagger\hat{a}_0|\Psi\rangle = N_0 = N\cos^2(\theta/2)$, $\langle\Psi|\hat{a}_1^\dagger\hat{a}_1|\Psi\rangle = N_1 = N\sin^2(\theta/2)$, and $\langle\Psi|\hat{a}_0^\dagger\hat{a}_1|\Psi\rangle = N|\alpha||\beta|\cos(\theta/2)\sin(\theta/2)\cos(\phi_1)e^{i\phi_2}$.

Using the wave-function ansatz (4), the total energy per particle reads [17]

$$\frac{E}{N} = \frac{N}{2}[U_0 + U_1 - 2P\cos(2\phi_2) - V]\sin^4(\theta/2) + \left[\epsilon_1 - \epsilon_0 + N\left(\frac{V}{2} - U_0 + P\cos(2\phi_2)\right)\right]\sin^2(\theta/2) + \frac{U_0}{2}N + \epsilon_0. \quad (5)$$

It is easily verified that, minimizing the above energy expression, we can recapture within one wave-function ansatz (4) the (continuum limit) observations made in [15] for the many-body ground states of the two-model (1). We will now discuss these quantum phases for the parameter regime $U_0 + U_1 + 2|P| - V > 0$ in more detail. For a numerical verification of the wave-function ansatz (4), see Sec. II C.

B. Coherence properties

The first-order coherence and degree of fragmentation $\mathcal{F}$ [15], corresponding to the ansatz (4), are, respectively, given by

$$g_1 = \frac{1}{2}\langle\hat{a}_0^\dagger\hat{a}_1 + \hat{a}_1^\dagger\hat{a}_0\rangle = 2|\alpha||\beta|\sqrt{N_0N_1}\cos(\phi_1)\cos(\phi_2) \quad (6)$$

and, using $\mathcal{F} = 1 - \frac{2}{N}|\frac{N}{2} - N_1|$,

$$\mathcal{F} = 1 - \frac{2}{N}\sqrt{|\langle\hat{a}_0^\dagger\hat{a}_1\rangle|^2 + \left(\frac{N}{2} - \langle\hat{a}_1^\dagger\hat{a}_1\rangle\right)^2} = 1 - \frac{2}{N}\sqrt{4|\alpha|^2|\beta|^2N_0N_1\cos^2(\phi_1) + \left(\frac{N}{2} - N_1\right)^2}. \quad (7)$$

For $P < 0$, the minimization of energy terms associated with the relative phase ϕ_2 in Eq. (5), $P\cos(2\phi_2)N_0N_1$, determines the phase to be either $\phi_2 = 0$ or π (mod 2π). Suppose that $\phi_1 = 0$ [this is achieved for $P < 0$ provided that an infinitesimally small Josephson-type coupling between the levels is present; cf. the discussion in Sec. III B and Eq. (17)] and $\phi_2 = 0$; the first-order coherence reads $g_1 = \sqrt{N_0N_1}$, implying that the ground-state phase is a *coherent* (single-condensate) state. On the other hand, when $\phi_2 = \pi$, the ground state is a *π-phase coherent* ground state, for which the system favors negative first-order coherence.

The second-order coherence function is defined by $g_2 = \frac{1}{2}\langle\hat{a}_0^\dagger\hat{a}_0^\dagger\hat{a}_1\hat{a}_1 + \hat{a}_1^\dagger\hat{a}_1^\dagger\hat{a}_0\hat{a}_0\rangle$. Evaluating it by using the ansatz (4) yields

$$g_2 = N^2\sin^2(\theta/2)\cos^2(\theta/2)\cos(2\phi_2) = N_0N_1. \quad (8)$$

The second-order coherence g_2 is independent of the relative phase ϕ_1 between coefficients α and β and is macroscopic, i.e., $O(N^2)$, implying that the ground-state is intrinsically *pair coherent* by virtue of energy minimization. By contrast, the first-order coherence g_1 depends on α and β, and proper coherent states in our model exist for $\alpha = \beta = 1/\sqrt{2}$ only. Minimizing the total energy with respect to $\sin(\theta/2)$, the occupation number in the "excited" single-particle state reads

$$N_1 = \langle\hat{a}_1^\dagger\hat{a}_1\rangle = \frac{\epsilon_0 - \epsilon_1 - \left(\frac{V}{2} - U_0 - |P|\right)N}{U_0 + U_1 + 2|P| - V}, \quad (9)$$

a formula also valid for $P > 0$.

Turning to positive pair-exchange coupling, minimal energy requires $\phi_2 = \pi/2$ or $-\pi/2$. This results in vanishing first-order and negative pair coherence, $g_1 = 0$ and $g_2 = -N_0N_1$. The ground state in the form of Eq. (4) can then be rewritten as follows:

$$|\Psi\rangle = \sum_{k=0}^{N/2} e^{\pm i\frac{\pi}{4}(N-4k)}[\alpha f_{2k}|2k\rangle \pm i\beta f_{2k+1}|2k+1\rangle], \quad (10)$$

where the real amplitude function f_k is defined by

$$f_k = \sqrt{\frac{2k!(N-k)!}{N!}}C_N^k[\cos(\theta/2)]^k[\sin(\theta/2)]^{N-k}, \quad (11)$$

and the upper and lower sign stands for $\phi_2 = \pi/2$ and $\phi_2 = -\pi/2$, respectively.

Macroscopic and negative pair coherence, vanishing first-order coherence, and, in particular, a finite degree of fragmentation $\mathcal{F}$ characterize the many-body state for $P > 0$ in our model and correspond to *fragmented* ground states.

C. Numerical verification of the wave-function ansatz

To verify the validity of our ground-state ansatz (4) for the two-mode model, we solve numerically the set of equations (2) when $|\alpha| = |\beta| = 1/\sqrt{2}$ to obtain ψ_l and compare it with

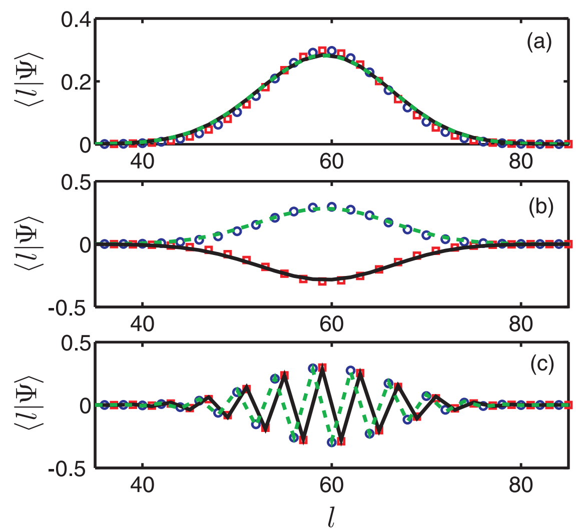

FIG. 1. (Color online) Comparison of numerics and the ansatz in Eq. (4). (a) The coherent state and (b) π-phase coherent state correspond to the parameters $U_0 = V = 1$, $U_1 = 0.8$, $P = -0.2$ while (c) the fragmented state is from $P = 0.2$ with other parameters identical to (a) and (b). $N = 100$, $\Omega = 0$, and $\epsilon_0 = \epsilon_1 = 0$ for all cases here. Based on numerically solving Eq. (2), the red squares indicate the even l sector of ψ_l, and the blue circles indicate the odd l sector. The black solid line and the green dashed line correspond to the even and odd l parts of the analytic formula for the distribution functions $\mathcal{P}(l)$, respectively.

the distributions $\mathcal{P}(l) \equiv \langle l|\Psi\rangle$,

$$\mathcal{P}(l) = \sqrt{\frac{N!}{(N-l)!l!}}u^{N-l}v^l \tag{12}$$

for coherent and

$$\mathcal{P}(l) = \begin{cases} \sqrt{\frac{N!}{(N-l)!l!}}u^{N-l}v^l & \forall\, l \text{ even},\\ \pm i\sqrt{\frac{N!}{(N-l)!l!}}u^{N-l}v^l & \forall\, l \text{ odd} \end{cases} \tag{13}$$

for fragmented states, respectively.

The results displayed in Fig. 1 show that the ansatz (4) is consistent with the numerical results based on Eq. (2), establishing the validity of our generic ground-state expression in the interacting two-mode model.

We now proceed to demonstrate the fundamental distinction between our fragmented states and fragile fragmented states by contrasting their respective responses to various perturbations, e.g., quantum fluctuations and Josephson-type couplings between the single-particle states.

III. STABILITY OF FRAGMENTED STATES AGAINST PERTURBATIONS

A. Quantum fluctuations of number and phase

We start by defining states which infinitesimally differ from the ground state by writing the former in terms of the spinor states $|\theta,\phi\rangle = |\theta_0 + \delta, \phi_2 + \phi\rangle$, where θ_0 and ϕ_2 determine, respectively, the particle number of the ground states in the two modes and the relative phase between $|l\rangle$ and $|l+2\rangle$.

Expanding up to quadratic order in δ and ϕ around the ground state corresponding to the minimum of (5) and using relation (9), we obtain that the low-lying excitations have the following energy, quadratic in phase (ϕ) and number (δ) fluctuations:

$$\begin{aligned} &E(\theta_0+\delta,\phi_2+\phi) - E(\theta_0,\phi_2)\\ &\quad = 2|P|N_0N_1\phi^2 + \left[\left(U_0 - \frac{V}{2} + |P|\right)\frac{3N_0N_1 - N_0^2}{4}\right.\\ &\qquad + \left(U_1 - \frac{V}{2} + |P|\right)\frac{3N_0N_1 - N_1^2}{4}\\ &\qquad \left. + (\epsilon_1 - \epsilon_0)\frac{N_0 - N_1}{4}\right]\delta^2. \end{aligned} \tag{14}$$

The crucial feature of the above result for the excited-state energy is that it makes explicit that the energy of quantum fluctuations depends only on the *absolute value* of the pair-exchange coupling $|P|$. Therefore, the presently considered fragmented state with continuous distribution amplitudes $|\psi_l|$, obtained sufficiently far from $P = 0$ (also see below), is as robust against fluctuations of the ψ_l distribution as a coherent state at the same value of $|P|$. Note in this respect that the factor N_0N_1 in front of ϕ^2 implies that the excitation energy per particle grows linearly in the total number of particles, so that the critical region of instability towards phase fluctuations around $P = 0$ has the size $\delta P \sim O(1/N)$ [18].

We now set the above discussion in relation to the analogous one for the well-known double well, as again described by a two-mode model [19], with a Hamiltonian

$$\hat{H} = -\frac{\Omega}{2}(\hat{a}_L^\dagger \hat{a}_R + \text{H.c.}) + \frac{U}{2}\sum_{i=L,R}\hat{n}_i(\hat{n}_i - 1), \tag{15}$$

in terms of the lowest-energy single-particle left and right eigenstates, putting $\epsilon_L = \epsilon_R = 0$. The energy in terms of the spinor wave functions (3) reads $E(\theta,\phi) = -\frac{\Omega}{2}N\cos\phi\sin\theta + U[\frac{N^2}{4}(\cos^2\theta + 1) - \frac{N}{2}]$. The excitation energy around the two-mode coherent state, $|C\rangle = (\hat{a}_0^\dagger + \hat{a}_1^\dagger)^N|0\rangle/\sqrt{2^N N!}$, in the double-well system therefore takes the form

$$E(\pi/2+\delta,\phi) - E(\pi/2,0) = \frac{\Omega}{4}N\phi^2 + \frac{N}{4}(\Omega + UN)\delta^2 + \cdots. \tag{16}$$

Comparing Eqs. (14) and (16), a pronounced difference is manifest: The energy of phase fluctuations is associated with $N_0N_1 \propto N^2$ for the fragmented many-body ground state of (1), while it is linear in the total particle number $N_0 + N_1$ in the double-well system.

Therefore, we come to the surprising conclusion that the single-trap fragmented state is *less* susceptible to phase fluctuations in the thermodynamic limit than its double-well counterpart, provided single-particle and pair-exchange amplitudes, Ω and $|P|$, for the double well and single trap, respectively, are approximately of the same order. This is reflected in the width of the critical region around $P = 0$ discussed above; there is no such critical region (critical in terms of the N scaling of the exchange or tunneling coupling) for stability against phase fluctuations in the double-well case.

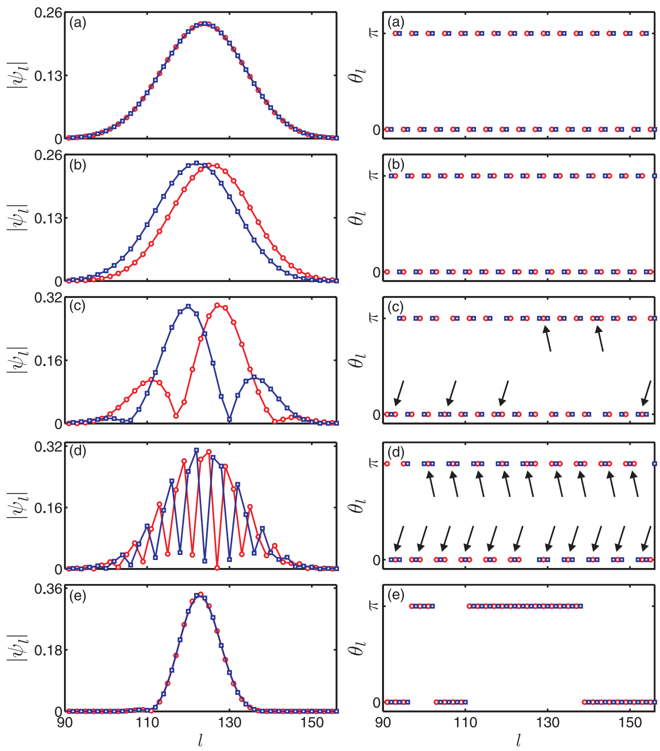

FIG. 2. (Color online) The Fock space distribution (left) amplitude $|\psi_l|$ and (right) phase θ_l of the ground-state wave function, varying the single-particle tunneling Ω, for a fragmented state with $P = 0.4$, $U_0 = V = 1$, $U_1 = 2/3$, $\epsilon_0 = \epsilon_1 = 0$, and $N = 200$. The Josephson-type coupling increases from top to bottom, (a) $\Omega = 0$, (b) $0.015NU_0$, (c) $0.1NU_0$, (d) $0.4NU_0$, and (e) $0.8NU_0$. Red circles represent the odd l sector, and blue squares show the even l sector. The arrows pointing to the phase data indicate the increasing breakup of the phase structure of the fragmented state. The phase structure of the ground state of (1), i.e., for $\Omega = 0$, alternates according to the scheme $(0,0,\pi,\pi,0,0,\pi,\pi,\ldots)$.

B. Josephson-type single-particle coupling

A Josephson-type perturbation of the form

$$\hat{H}_J = -\frac{\Omega}{2}(\hat{a}_0^\dagger \hat{a}_1 + \text{H.c.}) \tag{17}$$

couples the two modes on the single-particle level. This can be due to tunneling in the case of a double well, as discussed above. For a single trap, it can be realized by using two hyperfine states coupled by a two-photon Raman transition. The energy of such a perturbation in terms of the state (4) is

$$\begin{aligned} H_J &\equiv \langle \Psi | \hat{H}_J | \Psi \rangle \\ &= -\Omega N |\alpha||\beta| \cos(\theta/2)\sin(\theta/2)\cos(\phi_1)\cos(\phi_2). \end{aligned} \tag{18}$$

Minimizing the Josephson energy H_J yields $\alpha = \beta = 1/\sqrt{2}$ when $\Omega\cos(\phi_2) > 0$ and the two modes are both occupied macroscopically, i.e., $\sin(\theta/2) \neq 0$ and 1. For a coherent state where $\phi_2 = 0$, the Josephson-type energy is negative (the Josephson tunneling rate being positive definite, $\Omega > 0$). Single-particle tunneling reduces the total energy and stabilizes the coherent state. By contrast, the π-phase coherent state ($\phi_2 = \pi$) leads to the Josephson-tunneling energy H_J being positive, which indicates that the π-phase coherent state is unstable for any finite Ω.

When $\Omega = 0$, the coefficients α and β in the even-odd superposition (4) can be any choice, subject to $|\alpha|^2 + |\beta|^2 = 1$. However, the Josephson-type tunneling, even when infinitesimally small, pins down the explicit form of the pair-coherent states, in a similar manner to its establishing the conventional single-particle coherent states.

As mentioned in the Introduction, the fragmented many-body states found in previous work emerge at special symmetry points of the Hamiltonian in question and are either macroscopically occupied single Fock states [2] or Schrödinger's cat states consisting of the coherent superposition of macroscopically distinct single Fock states [20]. For the latter, the instability of this type of (maximally) fragmented state is manifest as small quantum fluctuations rapidly destroy fragile superpositions of the NOON type.

To illustrate and compare the stability features of both robust and Fock-state-type fragmented states, we produce them within our two-mode model by adjusting the pair-exchange coupling P close to zero and then examine their stability against Josephson-type perturbations.

As seen in Figs. 2(a) and 2(b), for a small $\Omega = O(0.01NU_0)$, the robust fragmented state with Gaussian-shaped distribution experiences only a small alteration: The distributions of even and odd l parts of $|\psi_l|$ slightly shift relative to each other, while the phase structure θ_l, in particular the crucial feature of π-phase jumps between even and odd l, remains unchanged. With increasing single-particle tunneling, for example, from $0.1NU_0$ [Fig. 2(c)] to $0.8NU_0$ [Fig. 2(e)], the smooth amplitude function develops increasing modulations, and the corresponding phase structure is broken gradually due to the competition between single-particle tunneling and pair-exchange coupling. Finally, a uniform phase is established, and the Gaussian distribution of the many-body wave function revives when the ground-state properties are largely dominated by a very large single-particle tunneling of the order of the interaction energy [$\Omega = O(NU_0)$; see Fig. 2(e)].

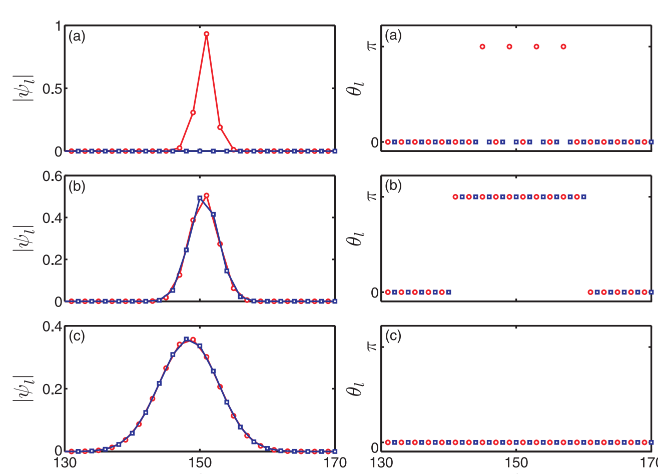

FIG. 3. (Color online) Evolution of a fragmented state which is "almost" a Fock state upon variation of the single-particle tunneling coupling Ω. We use parameters $P = 0.0001$, $U_0 = V = 1$, and $U_1 = 2/3$. In (a), $\Omega = 0$, while (b) and (c) represent the response to $\Omega = 0.003NU_0$ and $0.015NU_0$.

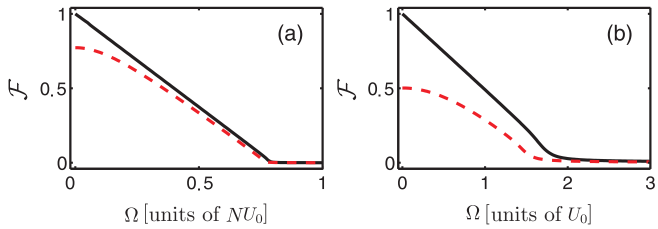

FIG. 4. (Color online) Variation of the degree of fragmentation with tunneling coupling for (a) a robust ($P = 0.4$) and (b) a fragile fragmented state with $P = 0.001$ [$= O(1/N)$]. Black: $U_0 = U_1 = V = 1$. Red (gray): $U_0 = V = 1$ and $U_1 = 2/3$; $\epsilon_0 = \epsilon_1 = 0$ and $N = 1000$. Note the macroscopically distinct scales on the Ω axis in (a) and (b).

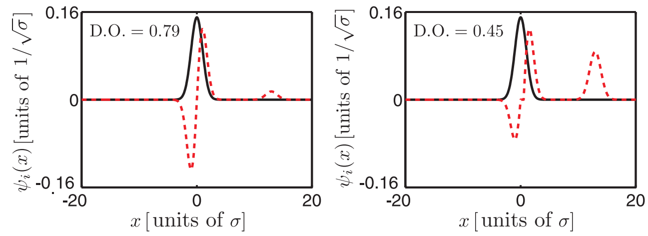

FIG. 5. (Color online) Examples for the deformation of the first excited state of the harmonic oscillator $\psi_1(x)$ (red dashed line) away from exact odd parity with varying degree of overlap. The ground state $\psi_0(x)$ is shown by the black solid line. The excited state with definite (odd) parity here corresponds to D.O. = 0.8.

By contrast, a comparatively small Josephson-type tunneling [for example, $\Omega = O(0.01NU_0)$] breaks a fragile fragmented state in the critical region around $P = 0$ [Fig. 3(a)], and the system is driven towards a coherent state [Fig. 3(b)]; the sharply peaked distribution and nonuniform phase structure for this fragile fragmented state rapidly evolve into a Gaussian distribution and a uniform phase structure with increasing Ω.

We summarize these properties in Fig. 4, which shows the variation of the degree of fragmentation upon increasing the single-particle tunneling and thus the conversion from a fragmented condensate to a single condensate. Figure 4(b) demonstrates that the (close to) Fock-like fragmented states quickly decay into a coherent state already for small Ω. On the other hand, the fragmented states with large distribution width ($P = 0.4$) are persistent, and a comparatively huge Ω [$O(NU_0)$], i.e., of the order of the interaction energy scale, is necessary to transform them to a coherent, single-condensate state.

C. Modes without definite parity

In general, there are interaction-induced terms of the form $-\frac{1}{2}J_2\hat{a}_0^\dagger\hat{a}_0^\dagger\hat{a}_0\hat{a}_1 + \text{H.c.} = -\frac{1}{2}J_2\hat{n}_0\hat{a}_0^\dagger\hat{a}_1 + \text{H.c.}$, as well as $-\frac{1}{2}J_2'\hat{a}_1^\dagger\hat{a}_1^\dagger\hat{a}_1\hat{a}_0 + \text{H.c.} = -\frac{1}{2}J_2'\hat{n}_1\hat{a}_1^\dagger\hat{a}_0 + \text{H.c.}$, in addition to those occurring in (1). This happens even in the presently considered case of a single trap, when the modes do not have a definite parity which is different for the two modes. On the other hand, when the modes respect a definite parity, the coefficients $J_2 = \int\int dx dx' V(x - x')[\psi_0^*(x)]^2\psi_0(x')\psi_1(x')$ and $J_2' = \int\int dx dx' V_{\text{int}}(x - x')[\psi_1^*(x)]^2\psi_1^*(x')\psi_0(x')$ are zero, where $V_{\text{int}}(x - x')$ is the two-body interaction, assumed to be of a definite parity. The terms $\propto J_2, J_2'$ lead to number-weighted tunneling-coupling processes. The corresponding weight in the energy scales with N^2J_2 and N^2J_2'; hence, when J_2 and J_2', respectively, are of the same order as P, these terms will have a significant influence on the degree of fragmentation $\mathcal{F}$, similar to a tunneling rate Ω of order NU_0.

We demonstrate now with a specific example that, in a single trap, we do not expect number-weighted tunneling to play a significant role when the parity of the modes is weakly broken. We take as the two (real) modes the ground state of the harmonic oscillator $\psi_0(x) = (\pi\sigma^2)^{-1/4}\exp[-x^2/2\sigma^2]$ and the first excited state $\psi_1(x) = (\sqrt{\pi}\sigma^3/2)^{-1/2}x\exp[-x^2/2\sigma^2]$ in one dimension and deform mode $\psi_1(x)$ away from odd parity by introducing, at an arbitrary position where $\psi_0(x)$ has no weight, an additional maximum of $\psi_1(x)$ (cf. Fig. 5), keeping in the process exact orthogonality, $\int dx\psi_0(x)\psi_1(x) = 0$, and normalization of the modes. To parametrize the change in the orbital's shape away from definite parity, we define the degree of orbital overlap as D.O. $\equiv \int dx|\psi_0(x)\psi_1(x)|$. When the degree of overlap tends to zero and the parity violation becomes large, we effectively have the familiar case of a double-well potential (see Fig. 5), which displays examples for the excited-state orbital when deformed away from the definite-parity state corresponding to the first excited state of the harmonic oscillator.

We then compute the coefficient ratios $J_2/P, J_2'/P$ for varying degrees of overlap. From Fig. 6, we conclude that as long as the degree of overlap remains large and parity of the modes is almost preserved, the fragmentation remains largely unaffected, while for larger $|J_2/P|, |J_2'/P|$, the effect of interaction-induced number-weighted tunneling on fragmentation will be, as expected, equivalent to a tunneling rate of order NU_0 [cf. Fig. 4(a)]. As long as parity is only weakly broken and $|J_2| \ll |P|$, stable fragmentation is thus still determined by the finite value of P. We expect weak breaking of parity, for example, when the trap confining the bosons does not exactly respect a definite parity. On the other hand, for maximally broken parity, pair exchange becomes less important than number-weighted tunneling, and the physics of an effective double well takes over.

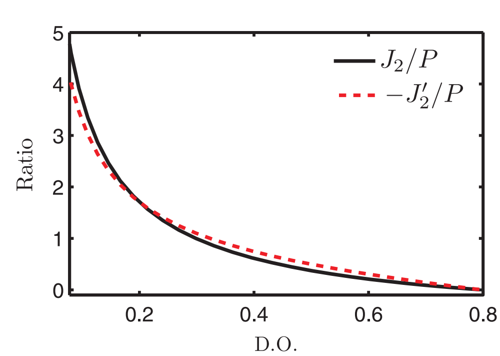

FIG. 6. (Color online) Ratios of coupling constants J_2/P, $-J_2'/P$ as a function of the degree of overlap of the orbitals. The degree of parity breaking increases from right to left. The ratios are identical, e.g., for a contact $V_{\text{int}} = g\delta(x - x')$ or a dipolar interaction $V_{\text{int}} = 3g_d/4\pi|x - x'|^3$.

D. Adding a third mode

We now study whether two-mode fragmented states continue to exist when a third mode, potentially also macroscopically occupied, couples to the two modes.

The three-mode Hamiltonian is in analogy to the two-mode case given by

$$\hat{H} = \sum_{i=0,1,2} \left[\epsilon_i \hat{n}_i + \frac{U_i}{2} \hat{n}_i(\hat{n}_i - 1) \right] + \frac{P_0}{2}(\hat{a}_0^\dagger \hat{a}_0^\dagger \hat{a}_1 \hat{a}_1 + \text{H.c.}) + \frac{P_1}{2}(\hat{a}_1^\dagger \hat{a}_1^\dagger \hat{a}_2 \hat{a}_2 + \text{H.c.}) + \frac{P_2}{2}(\hat{a}_0^\dagger \hat{a}_0^\dagger \hat{a}_2 \hat{a}_2 + \text{H.c.}) + \frac{V_0}{2}\hat{n}_0 \hat{n}_1 + \frac{V_1}{2}\hat{n}_1\hat{n}_2 + \frac{V_2}{2}\hat{n}_0\hat{n}_2, \quad (19)$$

where additional pair-exchange terms associated with the couplings P_1, P_2 as well as density-density-type terms $\propto V_1, V_2$ are included.

We set $\epsilon_i = 0$ for simplicity in what follows. The first-order coherence measures for the three modes are specified by

$$g_{ij}^{(1)} = \tfrac{1}{2}\langle \hat{a}_i^\dagger \hat{a}_j + \hat{a}_j^\dagger \hat{a}_i \rangle, \quad (20)$$

where $i, j = \{0,1,2\}$ labels the modes; in particular, $g_{01}^{(1)} \equiv g_1$, as defined in Eq. (6).

We start from a twofold fragmented state as a ground-state solution of the three-mode Hamiltonian above, with no (macroscopic) occupation in the third mode. To study the perturbative influence of the third mode, we then increase the pair-exchange couplings P_1 and P_2 simultaneously from zero to the same order as P_0, such that the particle number in the third mode increases gradually [cf. Fig. 7(a)]. We study the paradigmatic case shown in Fig. 7 because we anticipate, following the discussion in Sec. III B, that among the parameters associated with the third mode the pair-exchange parameters P_1 and P_2 influence the coherence properties of the many-body state most significantly. With increasing $P_1 = P_2$, both λ_2 and n_2 increase until a maximum of λ_2 occurs. At the same time, this maximum indicates the transition to a novel two-mode fragmented state, for which a finite coherence between modes $i = 0$ and $i = 2$ develops [see Fig. 7(c)]. That is, moving away from the small maximum in λ_2 towards larger values of P_1, λ_2 decreases from its small peak to zero again, and the threefold fragmented state converts again into a fragmented state with just two macroscopic eigenvalues of the single-particle density matrix instead of three. We verified that this behavior qualitatively also occurs if we keep, e.g., $P_2 = 0$ and only increase P_1. Whether either macroscopic $g_{02}^{(1)}$ or $g_{12}^{(1)}$ develops (limiting our discussion to $P_i > 0$) varies with the choice of parameters. For example, choosing $U_0 = 0.8$ and $U_1 = 1$ in Fig. 7, $g_{12}^{(1)}$ becomes macroscopic instead of $g_{02}^{(1)}$.

We thus conclude that the two-mode fragmented state can be stable against perturbations due to interaction coupling with a third mode, even when this mode also develops a significant (macroscopic) occupation.

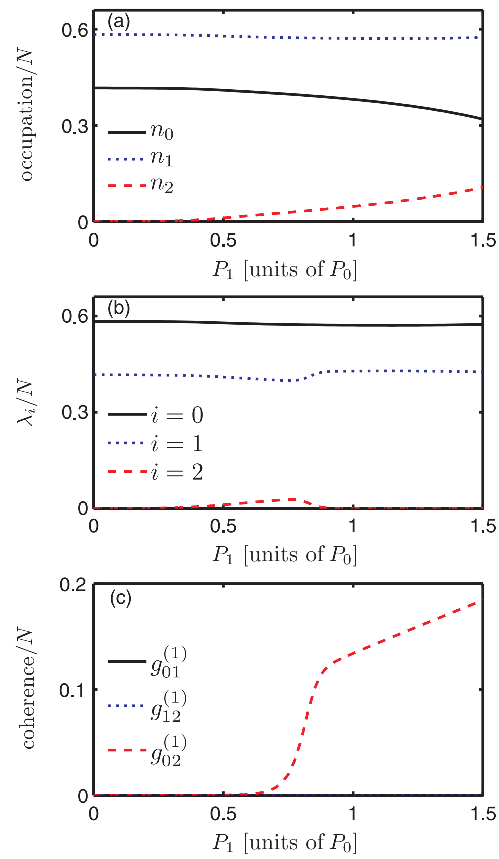

FIG. 7. (Color online) Illustration of the perturbative influence of an additional mode on a twofold fragmented state. We display the average occupation of the three modes in (a), the three eigenvalues λ_i of the single-particle density matrix in (b), and the first-order coherence measures (20) between various modes in (c), as a function of the pair-exchange tunneling P_1 between modes $i = 1$ and $i = 2$ in units of P_0. Here, $P_1 = P_2$ is fixed, and $U_0 = 1$, $U_1 = 0.8$, $U_2 = 1.2$, $V_0 = 1$, $V_1 = V_2 = 1.2$, and $N = 200$.

IV. CONCLUDING REMARKS

We have investigated whether fragmented states in a two-mode model with pair exchanges, representing bosons interacting by two-body forces in a single trap, are robust against perturbations of various origin.

We constructed an analytical ansatz describing the many-body solutions, which was verified numerically. Concentrating on a fragmented condensate solution originating from positive pair-exchange coupling, we reveal its persistence against quantum fluctuations of particle numbers in the modes and their relative phase, against single-particle tunneling and (weakly) broken parity of the modes, as well as the introduction of an additional interacting mode. A possible extension of the present work is to determine the spatial orbitals with multiconfigurational methods [21–23] and hence to solve the stability problem self-consistently. For example, fragmented condensates have been found in the crossover from a single condensate to "fermionization" [24], for tightly laterally confined bosons [25,26]. It would then be of interest to investigate the more generic situation where also the coupling coefficients in the Hamiltonian can (in principle significantly) vary upon perturbing the system and the ensuing consequences for the stability properties of fragmented condensates.

One might legitimately ask whether rising temperatures above absolute zero, as $T = 0$ was assumed in what precedes, destroy the fragmented condensate states. In the canonical ensemble, the thermal average of the operators occurring in the degree of fragmentation as defined in (7) is given by $\langle \hat{O} \rangle = \sum_{\gamma=0}^{N} \frac{e^{-\frac{E_\gamma}{T}}}{Z} \langle E_\gamma | \hat{O} | E_\gamma \rangle$, where the canonical partition sum $Z = \sum_{\gamma=0}^{N} e^{-E_\gamma/T}$ and $|E_\gamma\rangle$ are the eigenstates at energy E_γ. We have verified that increasing the temperature to very large values $O(NU_0)$ does not change the degree of fragmentation $\mathcal{F}$ significantly; there is only a slight change (on the subpercent level) for the parameter values used in Fig. 2. The fragmentation considered herein is therefore also not sensitive to finite-temperature effects.

In summary, the present study demonstrates that there exist robust fragmented condensate many-body states in a single trap, which share many features in regard to their stability with single-condensate states, for which it is well established that they are stable under (sufficiently small) perturbations.

ACKNOWLEDGMENTS

This research was supported by the NRF Korea, Grants No. 2010-0013103 and No. 2011-0029541.

[1] O. Penrose and L. Onsager, Phys. Rev. **104**, 576 (1956).

[2] E. J. Mueller, T.-L. Ho, M. Ueda, and G. Baym, Phys. Rev. A **74**, 033612 (2006).

[3] A. D. Jackson, G. M. Kavoulakis, and M. Magiropoulos, Phys. Rev. A **78**, 063623 (2008).

[4] R. W. Spekkens and J. E. Sipe, Phys. Rev. A **59**, 3868 (1999).

[5] D. Jaksch, C. Bruder, J. I. Cirac, C. W. Gardiner, and P. Zoller, Phys. Rev. Lett. **81**, 3108 (1998).

[6] B. P. Anderson and M. A. Kasevich, Science **282**, 1686 (1998).

[7] M. Greiner, O. Mandel, T. Esslinger, T. W. Hänsch, and I. Bloch, Nature (London) **415**, 39 (2002).

[8] T.-L. Ho and S. K. Yip, Phys. Rev. Lett. **84**, 4031 (2000).

[9] M. Koashi and M. Ueda, Phys. Rev. Lett. **84**, 1066 (2000).

[10] N. K. Wilkin, J. M. F. Gunn, and R. A. Smith, Phys. Rev. Lett. **80**, 2265 (1998).

[11] D. S. Rokhsar, arXiv:cond-mat/9812260.

[12] M. Ueda and A. J. Leggett, Phys. Rev. Lett. **83**, 1489 (1999).

[13] X. J. Liu, H. Hu, L. Chang, W. Zhang, S. Q. Li, and Y. Z. Wang, Phys. Rev. Lett. **87**, 030404 (2001).

[14] Q. Zhou and X. Cui, Phys. Rev. Lett. **110**, 140407 (2013).

[15] P. Bader and U. R. Fischer, Phys. Rev. Lett. **103**, 060402 (2009).

[16] U. R. Fischer, K.-S. Lee, and B. Xiong, Phys. Rev. A **84**, 011604(R) (2011).

[17] Note that we neglect in (5) and in the following equations $O(1/N)$ terms; however, we fully keep the single-particle energies, assuming their effective N scaling to be, in general, adjustable.

[18] The ansatz (4) for the wave function, with definite ϕ_2, is valid outside this critical region, i.e., when $P \gtrsim O(1/N)$. At $P = 0$, an equal-weight average over ϕ_2 yields an applicable wave-function ansatz (corresponding to a single two-mode Fock state), while away from $P = 0$, a (Gaussian) weighted average of (4) may be employed, analogous to the one performed in [2] for the single-particle tunneling Hamiltonian in Eq. (15).

[19] G. J. Milburn, J. Corney, E. M. Wright, and D. F. Walls, Phys. Rev. A **55**, 4318 (1997).

[20] T.-L. Ho and C. V. Ciobanu, J. Low Temp. Phys. **125**, 257 (2004).

[21] O. E. Alon, A. I. Streltsov, and L. S. Cederbaum, Phys. Rev. A **77**, 033613 (2008).

[22] J. Grond, A. I. Streltsov, L. S. Cederbaum, and O. E. Alon, Phys. Rev. A **86**, 063607 (2012).

[23] K.-S. Lee and U. R. Fischer, arXiv:1301.2199.

[24] M. D. Girardeau and E. M. Wright, Phys. Rev. Lett. **87**, 210401 (2001).

[25] O. E. Alon and L. S. Cederbaum, Phys. Rev. Lett. **95**, 140402 (2005).

[26] U. R. Fischer and P. Bader, Phys. Rev. A **82**, 013607 (2010).